Burns & Trauma, 2020, 8, tkaa009
doi: 10.1093/burnst/tkaa009
Research Article

Research Article

Adipose-derived stem cells improve grafted burn wound healing by promoting wound bed blood flow

Osamu Fujiwara[1,#], Anesh Prasai[2,3,#], Dannelys Perez-Bello[1], Amina El Ayadi[2–4], Irene Y. Petrov[5], Rinat O. Esenaliev[1,5,6], Yuriy Petrov[5], David N. Herndon[2,3], Celeste C. Finnerty[2–4], Donald S. Prough[1], and Perenlei Enkhbaatar[1,3,*]

[1]Department of Anesthesiology, University of Texas Medical Branch, Galveston, TX, USA, [2]Department of Surgery, University of Texas Medical Branch, Galveston, 301 University BLVD TX 77555, USA, [3]Shriners Hospitals for Children – Galveston, 815 Market Street Galveston, TX 77555, USA, [4]Sealy Center for Molecular Medicine, and the Institute for Translational Sciences, University of Texas Medical Branch, 301 University BLVD Galveston, TX 77555, USA, [5]Center for Biomedical Engineering, University of Texas Medical Branch, 601 Harbor Side Dr. Galveston, TX 77555, USA, and [6]Department of Neuroscience, Cell Biology, and Anatomy, University of Texas Medical Branch, 301 University BLVD Galveston, TX 77555, USA

*Correspondence. Email: peenkhba@utmb.edu
[#]These authors contributed equally to this work

Received 17 January 2020; Revised 22 January 2020; Editorial decision 22 January 2020

Abstract

Background: Researchers have explored the use of adipose-derived stem cells (ASCs) as a cell-based therapy to cover wounds in burn patients; however, underlying mechanistic aspects are not completely understood. We hypothesized that ASCs would improve post-burn wound healing after eschar excision and grafting by increasing wound blood flow via induction of angiogenesis-related pathways.

Methods: To test the hypothesis, we used an ovine burn model. A 5 cm^2 full thickness burn wound was induced on each side of the dorsum. After 24 hours, the burned skin was excised and a 2 cm^2 patch of autologous donor skin was grafted. The wound sites were randomly allocated to either topical application of 7 million allogeneic ASCs or placebo treatment (phosphate-buffered saline [PBS]). Effects of ASCs culture media was also compared to those of PBS. Wound healing was assessed at one and two weeks following the application of ASCs. Allogeneic ASCs were isolated, cultured and characterized from non-injured healthy sheep. The identity of the ASCs was confirmed by flow cytometry analysis, differentiation into multiple lineages and gene expression via real-time polymerase chain reaction. Wound blood flow, epithelialization, graft size and take and the expression of vascular endothelial growth factor (VEGF) were determined via enzyme-linked immunosorbent assay and Western blot.

Results: Treatment with ASCs accelerated the patch graft growth compared to the control ($p < 0.05$). Topical application of ASCs significantly increased wound blood flow ($p < 0.05$). Expression of VEGF was significantly higher in the wounds treated with ASCs compared to control ($p < 0.05$).

Conclusions: ASCs accelerated grafted skin growth possibly by increasing the blood flow via angiogenesis induced by a VEGF-dependent pathway.

Key words: Wound healing, Burn, Adipose-derived stem cells, Angiogenesis, Vascular endothelial growth factor, VEGF, blood flow

Background

With the fairly recent discovery of stem cells in adipose tissue, the use of adipose-derived stem cells (ASCs) to treat various ailments and diseases has become more frequent [1]. Before the discovery of ASCs, fat tissue removed during surgical procedures was routinely discarded. The potential utilization of ASCs as a wound healing therapy emerged after the latent stem cell properties of ASCs were disclosed by Zuk and colleagues [2]. With more than 15.6 million cosmetic procedures occurring every year, the procurement and isolation of ASCs have become a relatively easy process, due in part to the abundant availability of these cells [3]. Although many trials of the clinical utility of ASCs are ongoing, there is a dearth of work demonstrating how ASCs mediate and accelerate wound healing [4].

ASCs have similar wound healing properties and cytokine expression profiles as those of bone marrow-derived mesenchymal stem cells [5, 6]. The mechanisms by which ASCs, applied topically or injected subcutaneously, facilitate and accelerate wound healing are still largely unknown. Histological and flow cytometry studies have suggested that ASCs are located around the vascularized networks in fat tissue, in close proximity to pericytes and endothelial cells [7–9]. These ASCs secrete myriad growth factors involved in wound healing, including fibroblast grown factor, vascular endothelial growth factor (VEGF), hepatocyte growth factor, interleukin (IL)-6, IL-8, granulocyte colony-stimulating factor and granulocyte–macrophage colony-stimulating factor [4, 6, 10–12]. Through the action of these secreted proteins, ASCs can modulate the activities of endothelial cells, fibroblasts and other resident cells [13–15]. Among the various growth factors secreted by ASCs, VEGF has been well studied in small animal models, with limited data available from research in large animals or humans [16–22]. Modulation of endothelial cells by ASCs via paracrine or contact-dependent interactions may result in *de novo* vessel formation or increase the size of the blood vessels to accelerate wound healing. Furthermore, ASCs themselves can undergo endothelial differentiation under certain conditions [23], which may also contribute to the acceleration of wound healing.

We hypothesized that ASCs would improve post-burn wound healing after eschar excision and grafting by increasing wound blood flow through induction of angiogenesis-related pathways. In order to test the hypothesis, we used an established model of ovine burn wound healing. Endpoints included wound closure, graft growth as a measure of graft take, epithelialization, blood flow and expression of VEGF.

Methods

ASC isolation and culture conditions

All animal studies were conducted in adherence with the guidelines detailed in the NIH Guide for the Care and Use of Laboratory Animals. The study was reviewed and approved by the Institutional Animal Care and Use Committee of the University of Texas Medical Branch, Galveston, TX, USA.

Allogeneic adipose tissue was isolated from healthy sheep and washed extensively with phosphate-buffered saline (PBS) containing 5% penicillin/streptomycin. The tissue was then minced and incubated with 0.075% collagenase Type IA at 37°C for 70–90 minutes with constant shaking. Ovine adipose tissue contains a higher percentage of saturated fat compared to human adipose tissue, thus the duration of the enzymatic digestion was extended [24, 25]. Following complete digestion, an equal volume of complete media (Dulbecco's Minimum Essential Medium with 10% fetal bovine serum (FBS) and 2% antibacterial/antimycotic solution (10,000 IU/ml penicillin; 10,000 µg/ml streptomycin; 25 µg/ml amphotericin; 8.5 g/l NaCl)) was added in order to inactivate the collagenase. The solution was aspirated and centrifuged at 350 G for 5 minutes in order to separate the ASCs from the adipose tissue. The cell pellet was reconstituted with PBS and centrifuged at 350 G for 5 minutes. This step was repeated 3 to 4 times until the supernatant became clear. The pellet was then re-suspended in 4.5 ml of water for 30 seconds followed by the addition of 0.5 ml of 10X PBS in order to lyse the red blood cells. Complete media was then used to re-suspend the pellet and the solution was filtered through a 70 µm cell strainer, suspended in complete media, and washed twice with PBS. The final pellet was seeded into a 25 cm^2 tissue culture flask and incubated in 5% CO_2 at 37°C. After incubating for 18 hours, the media was replaced, removing the unattached cells and cellular debris. Cells were cultured and passaged until the second passage and frozen down in aliquots. At the fourth passage, the cells were used for the experiments.

Characterization of ASCs: differentiation and stemness-related marker detection

Ovine ASCs were characterized following the guidelines established by the International Society for Cellular Therapy and the International Federation for Adipose Therapeutics and Science [26] and previously published studies [27]. The primary isolates were cultured and passaged for expansion, to obtain the ASC-rich colonies and to preserve the aliquots for future experiments. The primarily cultured ASCs were frozen at the second passage. For differentiation, viability test, and application of ASCs, cells at the second passage

were thawed and again expanded until the fourth passage for the applications and experimentations. At the fourth passage, ASCs were differentiated into three different lineages to confirm stemness, while flow cytometry and semi-quantitative PCR were used to assess CD marker expression.

ASC differentiation

Following differentiation into three different lineages, as described below, the stained and differentiated ASCs were photographed using an inverted phase contrast microscope (Leica DFC450) at ×10 magnification.

Osteogenic differentiation In a 6-well plate, 10^4 cells per cm^2 were seeded in complete media. After 24 hours, the media was replaced with osteogenic differentiation media composed of complete media along with 0.1 µM dexamethasone, 50 µM ascorbate-2-phosphate, 3 mM NaH_2PO_4 [28] and 0.1 µM retinoic acid. Osteogenic differentiation was carried out for 28 days, with media changes performed every 3 days. Alizarin red staining was used to detect calcium phosphate, a marker of osteogenic differentiation.

Chondrogenic differentiation Cells were plated at a density of 10^5 cells per cm^2 for 24 hours in a complete media. The cells were placed on a rotary shaker at a lower setting for 5 minutes to concentrate the cells in the middle of the culture plates. After the cultures were confluent, cells were grown in chondrogenic differentiation media (Dulbecco's modified eagle medium [DMEM] with 6.25 µl/ml of insulin, 10 ng/ml of TGF-β, 50 nM ascorbate-2-phosphate and 2% FBS) for 28 days, with media changes performed every 3 days. Alcian blue staining was used to determine the degree of chondrogenic differentiation [29].

Adipogenic differentiation In a 6-well plate, 10^4 cells per cm^2 were plated in complete media for 24 hours. Differentiation was initiated by replacing complete media with adipogenic differentiation media (complete media with addition of 1 µM dexamethasone, 10 µM insulin, 0.5 mM isobutylmethylxanthine and 200 µM indomethacin). Cells were incubated in this media for 21 days, and the media changed every 3 days. Oil-red-o staining was used to evaluate adipogenic differentiation [2].

Cell surface marker detection via flow cytometry Fourth-passage ASCs were cultured in complete media until the cultures were 70–80% confluent. The cells were harvested with 0.25% trypsin/Ethylenediaminetetraacetic acid (EDTA). Cell viability was assessed via trypan blue staining. Analysis and determination of fluorescent cells, dead cells, debris and background noise were made with the BD Accuri™ C6 flow cytometer software. For CD marker staining, the cells were incubated in ice-cold PBS with 1% sodium azide for 15 minutes, washed three times with PBS and incubated with 3% BSA for 30 minutes on ice. Following 3 more PBS washes, aliquots of ASCs were incubated in 1% BSA per the manufacturer's guidelines with fluorescent dyes attached to the primary monoclonal antibodies for CD73, CD90, CD11b, CD34 and CD44.

Detection of mRNA transcripts via semi-quantitative PCR

In addition to flow cytometry, semi-quantitative PCR was used to detect the presence of transcripts for the CD markers used to confirm the ASC identity. Fourth passage commercially available human ASCs and laboratory-isolated ovine ASCs were utilized. Total RNA was isolated following the manufacturer's protocol (RNA isolation kit, Qiagen, Hilden, Germany). cDNA was made from the total RNA (iScript cDNA Synthesis Kit, Bio-Rad, Hercules, CA). The expression of stemness marker transcripts was analysed with semi-quantitative PCR using REDTaq® ReadyMix™ PCR Reaction Mix (Sigma, St. Louis, MO) using a DNA Engine® Peltier Thermal cycler. The primers used for the PCR reaction are listed in Table 1. The reaction products were electrophoresed on an agarose gel, which was photographed with the Syngene GeneGenius Bio Imaging System for visual comparison.

An ovine model of grafted burn wound healing

Surgical preparation Seven female sheep, weighing 27–37 kg, were housed in an animal facility with a 12-hour light and dark cycle for two weeks to acclimate prior to the initiation of the experiment. All animals received water and food *ad libitum* and were monitored for the entire duration of the study period.

After the acclimatization, the animals were transferred to the Translational Intensive Care Unit and chronically instrumented with multiple vascular catheters for cardiopulmonary hemodynamic monitoring, intermittent blood sampling, core body temperature and microsphere injection. Briefly, sheep were anesthetized with inhaled isoflurane (Piramal Healthcare Ltd., India) using an inhalation mixture of 2–5% in 60% oxygen, via endotracheal tube. Under aseptic conditions, a 7 Fr. Swan-Ganz thermodilution catheter (model 131F7; Edwards Critical Care Division, Irvine, CA) was inserted into the right jugular vein through an 8.5Fr. percutaneous introducer sheath (Edwards Lifesciences, Irvine, CA) and was advanced into the common pulmonary artery. Then, the right femoral artery was cannulated, and a polyvinylchloride catheter (16-gauge, 24-inch, Intracath; Becton Dickinson Vascular Access, Sandy, UT) was positioned in the descending aorta. Through a left thoracotomy at the level of the fifth intercostal space, a Silastic catheter (0.062-inch inner diameter, 0.125-inch outer diameter; Dow-Corning, Midland, MI) was positioned in the left atrium. Following the operative procedure, sheep were awakened and monitored in the Intensive Care Unit in a conscious state for 5–7 days. During this time, they had free access to food and water. Pre- and post-surgical analgesia was provided with buprenorphine (0.05 mg/kg, subcutaneous

Table 1. The list of primers used for determination of expression of stemness marker transcripts analysed with semi-quantitative PCR using REDTaq ReadyMix PCR Reaction Mix (Sigma, St. Louis, MO, US)

Gene	Forward primers	Reverse primers	Amplicon size
		Human	
Cyclophilin A	CTCGAATAAGTTTGACTTGTGTTT	CTAGGCATGGGAGGGAACA	165
CD34	TGGGCATCGAGGACATCTCT	GATCAAGATGGCCAGCAGGAT	107
CD11b/c	CTTGCCTTTCACCACCTGAT	TCCCAGGCTCCAGTATTTTG	208
CD73	CAGACTCATGATGACAGAGG	GAGATGTACAGGATCTTCCC	122
CD90	CACCAGTCACAGGGACATGA	ACCTACACGTGTGCACTACCA	192
CD105	CGTGGACAGCATGGACC	GATGCAGGAAGACACTGCTG	145
CD44	CAGGAAGAAGGATGGATATGG	ATTACTCTGCTGCGTTGTC	105
		Sheep	
Cyclophilin A	CATACAGGTCCT GGC ATC TTG TC	TGC CAT CCA ACC ACT CAG TCT	56
CD34	TGGGCATCGAGGACATCTCT	GATCAAGATGGCCAGCAGGAT	107
CD11b/c	CCTTCATCAACACAACCAGAGTGG	CGAGGTGCTCCTAAAACCAAGC	124
CD73	TGGTCCAGGCCTATGCTTTTG	GGGATGCTGCTGTTGAGAAGAA	115
CD90	CAGAATACAGCTCCCGAACCAA	CACGTGTAGATCCCCTCATCCTT	96
CD105	CGGACAGTGACCGTGAAGTTG	TGTTGTGGTTGGCCTCGATTA	115
CD44	GTGTCGTGTGCCCAGTTATGA	CTCGTCAGAGGTCCCATTTTC	511

Buprenorphine SR^{TM}, SR Veterinary Technologies, Windsor, CO).

Experimental protocol After 5–7 days of surgical recovery, sheep were again anesthetized with intravenous ketamine. Anesthesia was then maintained with 2–5% isoflurane in 60% oxygen. Two burn sites of approximately 25 cm^2 (5×5 cm each) were made on each side of dorsum with 7 cm between sites and 5 cm from the spine, yielding 4 wounds per animal. All four wounds covered ∼2% of the total body surface area. The burns were induced with a Bunsen gas burner until the skin was thoroughly contracted. During and after the burn procedure, until the surgery, all sheep were resuscitated with Ringer's lactate solution and had free access to water.

Twenty-four hours after induction of burn sites, under anesthesia (inhaled isoflurane) and analgesia (IV buprenorphine), the burned skin was excised to the level of the panniculus carnosus according to the clinical protocol for early excision established for human patients with third-degree burns. The average size of the resulting defect was approximately 25 cm^2 for each site.

Wounds were autografted with 2×2 cm skin patches. The autograft was harvested from the dorsum as split-thickness skin grafts (0.4 mm thickness) with an air dermatome. After the grafting procedure, the four wound sites were randomly allocated to the following: (1) one site (at one of the dorsum sides) was topically treated with 7 million ASCs reconstituted in 1 ml of vehicle (PBS); (2) another site (at one of dorsum sides) was topically treated with ASCs culture media; and (3) the remaining two sites were treated with PBS and served as controls at the contralateral dorsum side of either ASCs site or the media site. Each patch was attached by suturing in the center of the wound. The topically applied ASCs were allowed to equilibrate in the wound site for 10 minutes before the application of petroleum jelly. The ASC, culture media or PBS was topically applied, using a pipette, to the entire wound including the grafted patch graft. Aliquots were also applied underneath the patch graft.

After the treatment, the grafted wounds were covered with sterile non-adhesive polyurethane sheets and pressure bandages. The pressure bandage was removed on day 7 and the wounds were monitored for another week. During that time period, the wounds were covered with petroleum jelly and polyurethane to keep them moist. On the 15th day, sheep were euthanized under deep anesthesia and the wound tissues were sampled. Cardiopulmonary hemodynamic variables, such as heart rate, mean arterial blood pressure and mean pulmonary arterial pressure were monitored to ensure the wellbeing of the sheep. The core body temperature was also recorded.

Wound planimetry After the initial autografting and during each dressing change, standardized digital photographs of the wound sites were taken with a calibrated benchmark positioned adjacent to the wound. Photographs were analysed using planimetric software (Image J 1.43u, Wayne Rasband, National Institutes of Health, USA) to determine total wound size and the area of grafted skin at days 7 and 15.

Wound blood flow measurement using laser Doppler Blood flow in the treated and untreated wounds was measured using a laser Doppler device (PeriFlux System 5000 ModelPF5001, PERIMED) at 7 and 15 days after grafting as previously described [30]. Five locations (center and four corners of each site) were randomly chosen for measurement and the means were analysed.

Wound blood flow measurement using microsphere injection technique The wound blood flow was also measured by fluorescent microsphere injection. Approximately 5 million (two different colors) stable microspheres (15.0 ± 0.1 μ in diameter; Interactive Medical Technologies LTD, Los Angeles,

CA) were injected into the left atrium of the heart at day 0 (before burn induction), and 7 and 15 days after the skin grafting, as previously described [31]. 20 ml of blood was collected from the femoral artery within 2 minutes of injection with a Harvard pump (Harvard Apparatus Co. Model 55–1143, South Natick, MA) for the reference sample. At 15 days, sheep were euthanized and the wound was excised and the number of microspheres was counted in 1 g of tissue. Then, the blood flow was calculated as ml/g tissue per minute.

Ultrasound examination of autografted burn wounds The epithelialization of treated or untreated wounds was examined with high-resolution ultrasound (Vevo 2100 High-Resolution imaging system, VisualSonics), 7 and 15 days after grafting. The degree of epithelialization was scored as follows: score of 0: incomplete epithelialization; score of 1: partial epithelialization; score of 2: completed epithelialization with irregular and uneven epithelium; and score of 3: completed epithelialization with regular and even epithelium. Nine locations were randomly chosen for ultrasound measurements and the means were summarized.

Histological epithelialization score

The degree of uncovered wound epithelialization was assessed in formalin-fixed wound tissue by two independent and masked pathologists using light microscopy at 15 days after burn induction or skin grafting.

Quantitation of the VEGF protein Expression of the VEGF protein in the wound tissue was measured using enzyme-linked immunosorbent assay (ELISA). The ELISA was performed according to the manufacturer's instructions (Blue Gene Biotech, Shanghai, China). Tissue samples were also digested in protein lysis buffer and Western blot was performed on cultured ovine ASCs, PBS-treated sites (control) and ASC-treated sites (treatment), as previously described [27].

Statistical analysis

Prism 6 was used as the statistical analysis method. No differences were observed between PBS-treated sites and ASC-media treated sites at both the time points. The following statistical tests were used where appropriate: analysis of variance followed by Tukey's test; paired or unpaired Student's *t*-tests. Data are expressed as mean ± standard error of the mean. Significance was accepted at $p < 0.05$.

Results

Characterization of ovine ASCs

Cultured ovine, (Fig. 1a) as well as human (Supplementary Fig. 1), ASCs successfully differentiated into adipogenic,

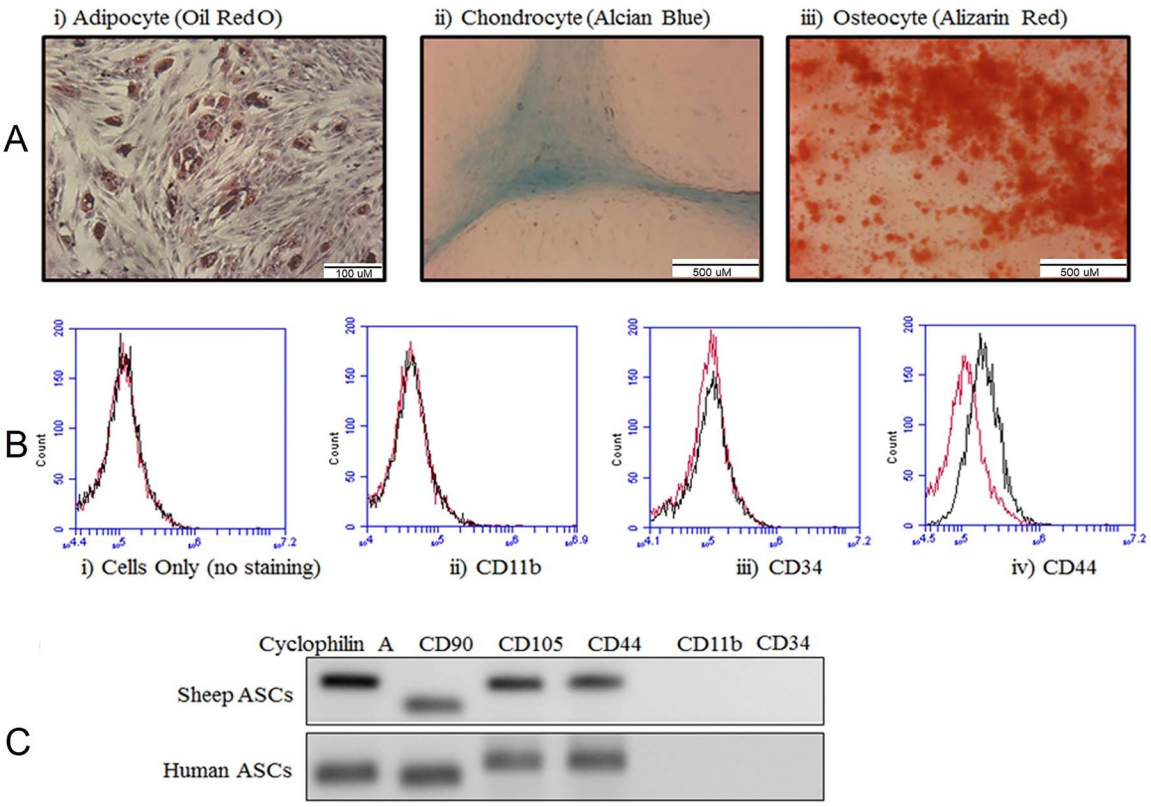

Figure 1. Characterization of ovine adipose-derived stem cells (ASCs). (**a**) ASCs were differentiated into three different lineages and stained for (i) adipocytes with oil-red-o, scale bar: 100 μM; (ii) chondrocytes with Alcian blue, scale bar: 500 μM; and (iii) osteocytes with Alizarin red, scale bar: 500 μM. (**b**) Characterization of ASCs with flow cytometry (i) isotype control (ii) CD11b, (iii) CD34 (iv) CD44. (**c**) mRNA transcript abundance for CD markers in ovine and human ASCs

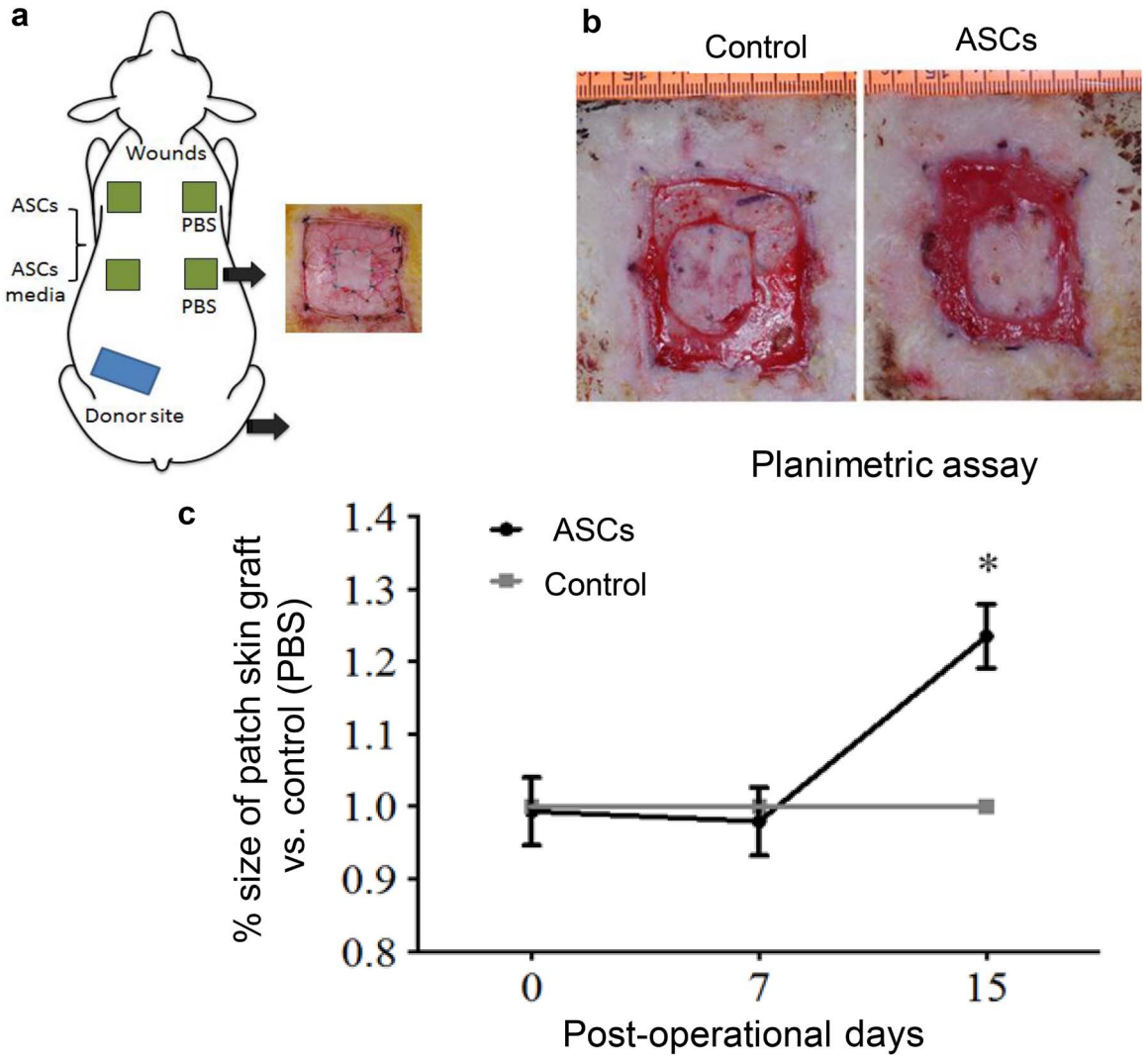

Figure 2. Graphical representation and quantification of sheep wound healing model. (**a**) Full thickness burns were induced in an area of 5 × 5 cm, with a total of four wounds per animal. (**b**) Pictorial representation of wound healing at day 15. (**c**) Graph depicts planimetric quantification of size of the skin graft at days 7 and 15 following the application of ASCs. The size of the ASC-treated graft is normalized to the size of the placebo-treated grafts. Error bars represent the standard error of the mean (n = 5, $*p < 0.05$, two-way analysis of variance). *ASCs* adipose-derived stem cells

chondrogenic and osteogenic lineages as shown by oil-red-o, Alcian blue and Alizarin red staining, respectively. Due to the lack of ovine antigen-recognizing antibodies for CD90, CD73 and CD105, only CD44 was detected on the ASCs via flow cytometry (Fig. 1b). Expression of mRNA transcripts for CD73, CD90, CD105 and CD44 was comparable in the ovine ASCs as compared with expression in commercially available human ASCs (Fig. 1c Commercial human ASCs differentiated into different lineages).

ASCs improved graft take and graft size

Although no differences were observed in the size of the skin graft at 7 days post-operation (Fig. 2), planimetry demonstrated that the graft size in ASC-treated wounds was significantly greater compared to control wounds at 15 days post-operation ($p < 0.05$) (Fig. 2c). The ratio of graft size in the ASC-treated to control wounds was 1.23 ± 0.12. Graft size was normalized to PBS control. No difference was noted between culture media and control groups, thus the data on culture media group is not shown.

ASCs significantly increased wound blood flow

Blood flow measured by laser Doppler in the ASC-treated wounds was normalized to the control-wound blood flow. Following ASC application, blood flow was significantly greater in ASC-treated wounds 7 days post-application (ASC-treated: $204.8 \pm 99.7\%$ compared to control: 100%, $p < 0.0025$), and tended to be higher 15 days post-application (ASC-treated: $167.2 \pm 39.6\%$ compared to control: 100%, $p < 0.0545$) (Fig. 3a).

The blood flow measured by microsphere injection technique was significantly higher at 15 days in the ASC-treated

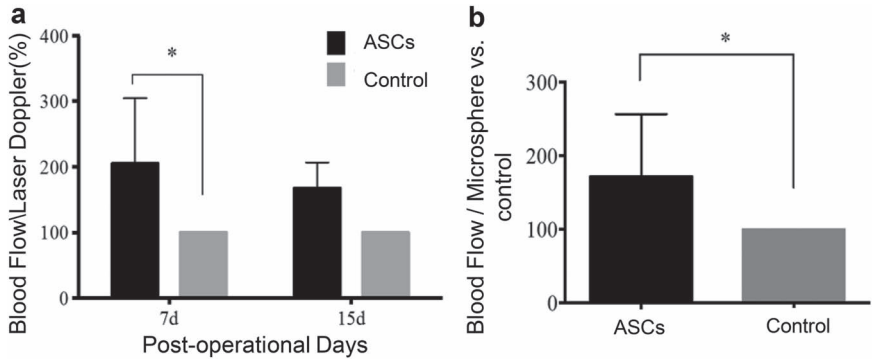

Figure 3. Adipose-derived stem cells (ASCs) significantly increased blood flow to the wound bed. (**a**) Measurement of blood flow by laser Doppler at days 7 and 15 (two-way analysis of variance). (**b**) Fluorescent microsphere injection technique. Error bars represent standard error of the mean (n = 7, $^*p < 0.05$, Mann-Whitney *U* test)

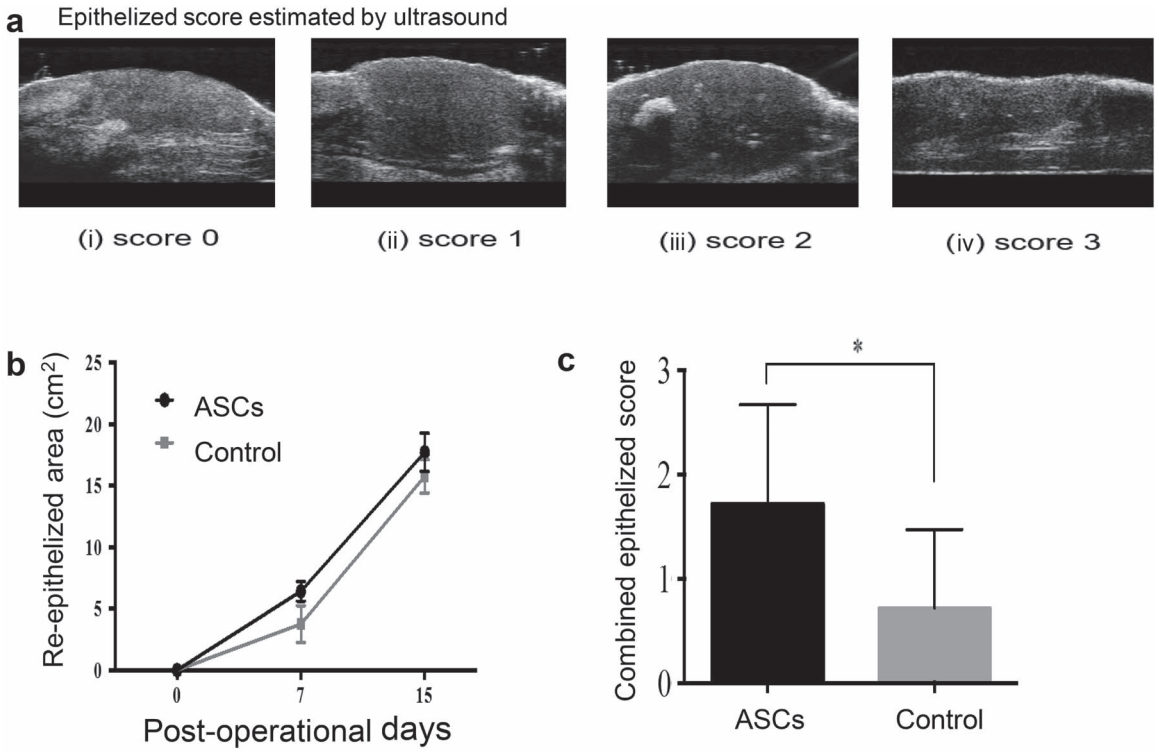

Figure 4. Topical application of adipose-derived stem cells (ASCs) increases wound epithelialization as measured by high-resolution ultrasound. (**a**) Epithelized area estimated by ultrasound: (i) score 0 = incomplete epithelialization; (ii) score 1 = partial epithelialization; (iii) score 2 = complete epithelialization with irregular and uneven epithelium; (iv) score 3 = complete epithelialization with regular and even epithelium. (**b**) Re-epithelized area measurement at 7 and 15 days after application of ASCs. Analysis of wound re-epithelialized determined by high-resolution ultrasound. (**c**) Combination of wound epithelialization score from both 7 and 15 days determined by high-resolution ultrasound (n = 6, $^*p < 0.05$, unpaired *t* test). Error bars represent standard error of mean

wounds (171.4 ± 85.2% compared to 100% in the controls, $p < 0.0169$) (Fig. 3b). The culture media treatment did not significantly affect the wound blood flow.

Wound epithelialization by ultrasound exam

The extent of epithelialization (white demarcation on top of the epidermis) was estimated by high-resolution ultrasound. Scores were given based on the extent of epithelialization: a score of 0 indicates incomplete epithelialization while a score of 3 indicates regular and complete epithelialization (Fig. 4a). There was no significant difference in the re-epithelized area at 7 and 15 days post-burn (Fig. 4b). However, when two time points were combined, the wound epithelialization scores were significantly higher in treated sites (1.71 ± 0.95) compared to control sites (0.71 ± 0.75), $p < 0.05$) (Fig. 4c). There was no difference found between media and PBS groups.

Comparable histological evidence of wound healing

Fig. 5a illustrates hematoxylin- and eosin-stained representative pictures of ASC-treated sites and control sites. There was

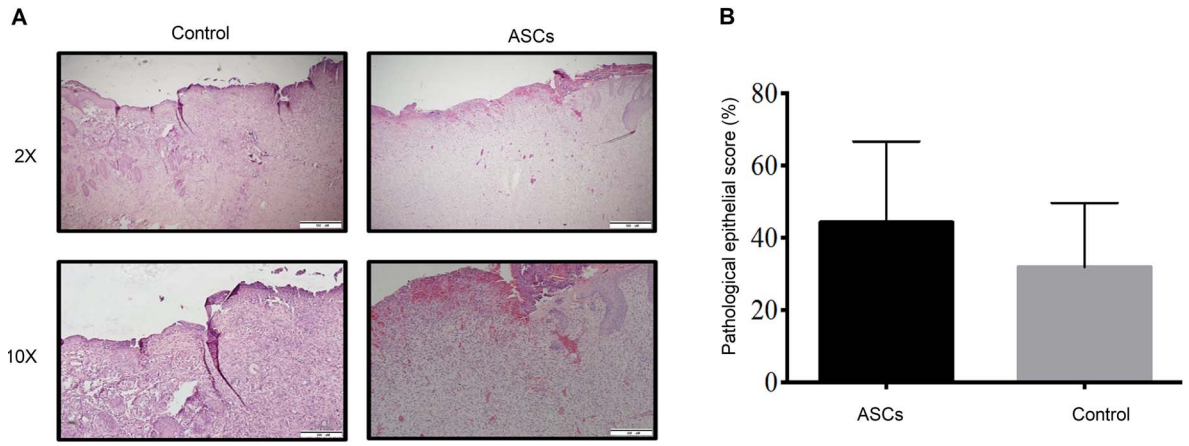

Figure 5. Histological examination and quantification of ASCs treated sites compared with the controls. (**a**) Representative histological sections of non-excised skin, PBS (control), and ASCs (treatment). First row ×2 magnification, scale bar: 500 μM; second row ×10 magnification, scale bar: 200 μM. (**b**) Quantification of histological scoring on ASC-treated and control sites at day 15. Error bars represent standard error of the mean. *ASCs* adipose-derived stem cells, *PBS* phosphate-buffered saline

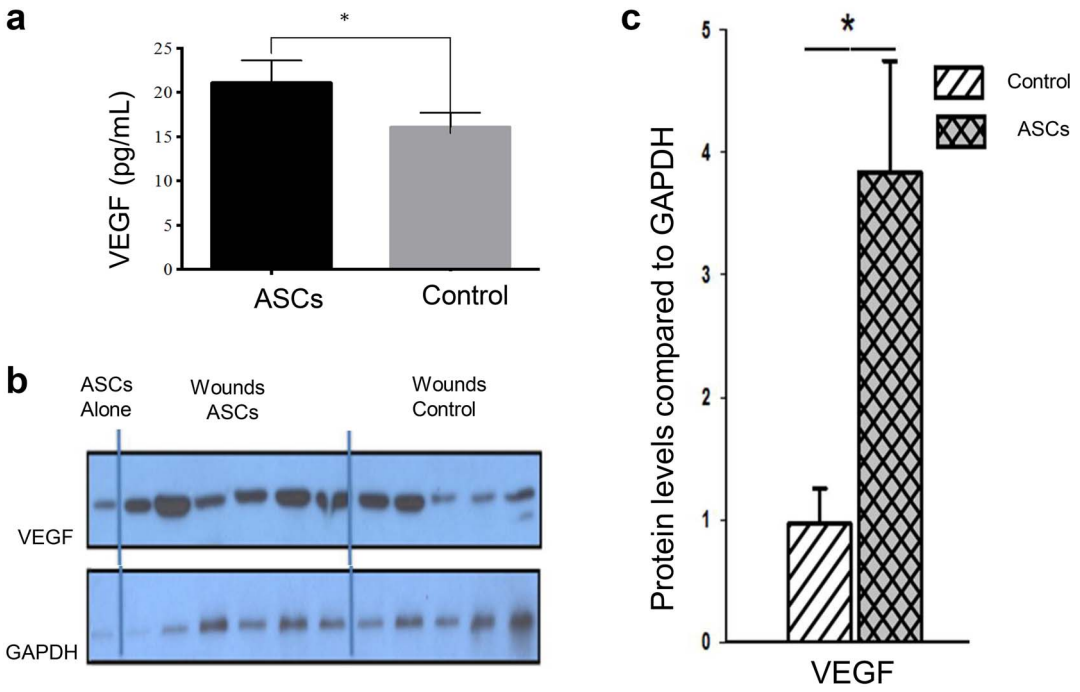

Figure 6. Wound bed VEGF expression is elevated with ASC treatment. (**a**) Wounds treated with ASCs express significantly more VEGF as measured by ELISA (n = 7, $^{*}p < 0.05$, Wilcoxon test). (**b**) Western blot staining for VEGF. First lane represents sheep ASCs, next six lanes represent treatment (n = 6) and the remaining 5 lanes represent PBS control (n = 5). (**c**) Semi-quantitative score of VEGF protein. Error bars represent standard error of mean ($^{*}p < 0.05$, unpaired *t* test). *ASCs* adipose-derived stem cells, *VEGF* vascular endothelial growth factor, *ELISA* enzyme-linked immunosorbent assay, *PBS* phosphate-buffered saline

no significant difference in re-epithelialization, as determined by histological examination between ASC-treated wounds (44.2 ± 9.2%) and control wounds (31.8 ± 7.3%) (Fig. 5b).

Wound bed VEGF expression is elevated with ASC treatment

Wound biopsy tissue obtained from vehicle- (PBS) and ASC-treated wounds 15 days post-application were pooled and VEGF levels were measured. ASC treatment resulted in significantly higher levels of VEGF compared to vehicle treatment (21.1 ± 2.5 pg/ml compared to 16.1 ± 1.7 pg/ml, respectively; $p < 0.05$) (Fig. 6a). Wound biopsies were also measured for VEGF with Western blot (Fig. 6b, c) and glyceraldehyde 3-phosphate dehydrogenase was used as a loading control ($p < 0.05$).

Discussion

The study was designed to evaluate the potential of allogeneic ASCs for healing grafted burn wound closure. Here, we first demonstrate beneficial effects of topically applied ASCs

on grafted burn wound healing in a novel ovine model. The wound care (escharectomy, wound closure and daily care) mimicked the clinical care provided to severely burned patients at our own institution. The sheep is a good alternative to other pre-clinical models typically used for wound healing studies, such as porcine models, in that sheep are easy to work with, do not require full sedation for all manipulations and the established model is clinically relevant. The novel ovine model of burn wound healing enables us to mimic a clinical situation: escharectomy, grafting, intermittent blood and wound biopsy sampling and intermittent wound assessment (blood flow by laser Doppler, photography for planimetry assay) without sedation. These interventions are not feasible in small animals and are difficult in pigs as sedation is necessary for all manipulations. The model has been presented several times at the major critical care meetings, including the American Burn Association meeting, and the model has been peer-reviewed and published [30]. Our ovine model has aspects of similarity to human burn wound healing that makes it appealing for these studies, including caring for the grafted wound in a conscious patient, contraction of the excised burn wound, growth of granulation tissue, the survival of the grafted skin and epithelialization from the grafted skin.

The beneficial effects of stem cell therapy on angiogenesis have previously been reported. Studies done by Kondo *et al*. on hind limb ischemic C57BL/6 J mice have demonstrated that the application of ASCs increases angiogenesis via an increase in stromal cell-derived factor 1 (SDF-1) mRNA and serum SDF-1 levels [32]. The majority of the studies elucidating the effects of ASCs on wound healing have utilized either ischemic or diabetic rat models to study vasodilation and neovasculogenesis. However, there is a paucity of research regarding how ASCs or other stem cells modulate the wound environment in relevant large animal models [33–35].

Recently, Burmeister *et al*. reported that topically applied ASCs in combination with PEGylated fibrin hydrogels increased wound blood vessels and CD31 staining in the pre-clinical Yorkshire model [36]. However, to our knowledge, no studies investigated the effects of ASCs on grafted burn wound healing in an ovine burn excision and grafted wound model.

ASCs are believed to have great potential for improving wound healing. Like bone marrow-derived mesenchymal stem cells, ASCs can regulate critical processes involved in wound healing, including inflammation [37–39], vascularity [11, 14] and immunity [40, 41]. Severe burn injury induces a hypermetabolic, hypercatabolic state, activating inflammation, vascular abnormalities and immune suppression. In patients with extensive burn injuries, sufficient donor skin for wound coverage may not exist, therefore use of ASCs may be a better option for enhancing wound healing following a severe burn injury [42, 43].

The main findings of the study were that ASCs, but not ASC culture media, accelerated growth of grafted skin and increased wound bed blood flow. ASCs promoted protein expression of the growth factor VEGF. Our data suggest that topically applied ASCs may have accelerated the growth of grafted skin by promoting wound bed blood flow. The increase in the blood flow around the wound bed may be attributed to an increase in the expression of the VEGF protein. Previous studies have elucidated the angiogenic influence of ASCs in different wound healing [35] and ischemic [11, 14] models. The increase in blood flow around the wound sites could be due to either the presence of more blood vessels or increased vasodilation; the end result of either of these scenarios is an increase in the blood volume circulating around the wound site. Following severe burn injury, there is extensive damage to the blood vessels. Additionally, there is an increase in demand for oxygen and nutrients to fuel the reparative and remodeling processes, defense mechanisms and debris clearance, resulting in greater demand for nutrients. The distress signals triggered by a burn injury within the wound niche may have activated the applied ASCs, as stem cells are known to modulate inflammation and angiogenesis processes [44]. Depending on the surrounding niche, ASCs may change from a pro- to anti-inflammatory phenotype. Thus, applied ASCs may be induced to release signals which can modulate the behavior of endothelial cells and other neighboring cells [45]. Additionally, other researchers have also observed an increase in angiogenesis following the application of ASCs or ASC-conditioned media in different burn and wound healing models [46–48].

One of the major limitations of the model used in this study is the constitutive wound contracture in the sheep. However, the impact of this issue was limited by comparing the wound contracture in the ASC-treated sites to the placebo-treated wounds. Comparisons were made between wounds located in similar anatomical regions (contralateral locations). Thus, there was no comparison made between ASCs and culture media sites. The duration was limited to only 15 days. Other limitations included the lack of appropriate anti-sheep antibodies for the quantification of the cell surface marker proteins, necessitating reliance on mRNA transcript abundance for the characterization of the ASCs. Another limitation of the study is that we did not clarify whether the theraputic effects of ASCs on wound healing are derived from paracrine effects of the proteins secreted by the ASCs as opposed to the ASCs differentiating into other cell types needed for wound healing. The use of tagged ASCs would have made the study more focused and would have also helped us to elucidate the molecular mechanism behind the role of ASCs in wound healing. Furthermore, tagged ASCs would have also helped us to answer whether the paracrine of the differentiating properties of ASCs aids in wound healing. However, we were unable to trace the dye-labeled ASCs in the IHC sections in our previous study, thus, in this present study, we avoided the use of dye to track the applied ASCs, which is one of the limitations of our study. Finally, although the grafting method is different than the meshed grafts applied to human patients, the grafting of unmeshed grafts was purposely selected in order to allow us to monitor graft take, the

survival of the tissue and proliferation of cells at the edges that expanded the area covered by the graft. Further limitations are related to the lack of data (including data using sophisticated histological methods) explaining underlying mechanisms of beneficial effects of topically applied ASCs. Future studies are warranted to determine the effects of ASCs on particular signaling cascades that underlie angiogenesis and wound healing.

In our animal study, following the topical application of ASCs to the grafted wound, there was a significant increase in VEGF protein expression, which may indicate that angiogenesis or vasodilation is the process responsible for increased blood flow. ASCs secrete growth factors known to modulate angiogenesis [6, 13]. Dynamic interaction between the ASCs and the surrounding niche can stimulate the production of growth factors that drive wound healing and regeneration. Nevertheless, our study supports the knowledge that ASCs aid in wound healing by increasing the blood flow.

Conclusions

The application of ASCs to burn wounds allows the wounds to heal faster. The blood flow to ASC-treated wounds is also greater. Future studies are warranted to elucidate the molecular mechanisms underlying how ASCs improved the healing of grafted burn wounds. Our data suggest that the topical application of ASCs improved grafted burn wound healing by promoting wound bed blood flow and increased VEGF protein expression.

Supplementary material

Supplementary material is available at *Burns & Trauma Journal* online.

Abbreviations

ASCs: Adipose-derived stem cells; VEGF: Vascular endothelial growth factor; IL: Interleukin; PBS: Phosphate-buffered saline; PCR: Polymerase chain reaction; RNA: Ribonucleic acid; SDF-1: Stromal cell-derived factor-1

Funding

This project was supported by grants from: the Shriners Hospitals for Children 84050 to PE and 84202 to AEA; the National Institutes of Health to DNH (R01-GM56687 and P50-GM-60338) and to CCF (R01-GM-112936); the Anderson Foundation and the Gillson Longebaugh Foundation to DNH and CCF. The project was conducted with the support of the University of Texas Medical Branch's Institute for Translational Sciences, supported in part by a Clinical and Translational Science Award (UL1TR000071) from the National Center for Advancing Translational Sciences (NIH).

Availability of data and materials

The data have not been published elsewhere. The abstract was presented at Tissue Engineering and Regenerative Medicine International Society conference 2014.

Authors' contributions

PE, CF, DH and DSP developed concept and planned the experiments. AP, OF, AE, DP, IP, RE and YP carried out the experiments. OF, AP and AE contributed to sample preparation. All authors provided critical feedback and helped to analyse data and prepare the manuscript. OF and AP contributed equally to this manuscript.

Ethics approval and consent to participate

The study was conducted adhering to guidelines established by the International Council for Laboratory Animal Science and the protocol was approved by the Institutional Animal Care and Use Committee.

Conflicts of interest

None declared.

References

1. De Francesco F, Ricci G, D'Andrea F, Nicoletti GF, Ferraro GA. Human adipose stem cells: From bench to bedside. Tissue Eng Part B Rev. 2015;**21**:572–84.
2. Zuk PA, Zhu M, Ashjian P, De Ugarte DA, Huang JI, Mizuno H, *et al.* Human adipose tissue is a source of multipotent stem cells. Mol Biol Cell. 2002;**13**:4279–95.
3. American Society of Plastic Surgeons. ASPS National Clearinghouse of Plastic Surgery Procedural Statistics. 2014 Plastic Surgery Statistics Report. https://www.plasticsurgery.org/documents/News/Statistics/2014/plastic-surgery-statistics-full-report-2014.pdf. Accessed 1 Nov 2019.
4. Wang M, Crisostomo PR, Herring C, Meldrum KK, Meldrum DR. Human progenitor cells from bone marrow or adipose tissue produce VEGF, HGF, and IGF-I in response to TNF by a p38 MAPK-dependent mechanism. Am J Physiol Regul Integr Comp Physiol. 2006;**291**:R880–4.
5. Heo JS, Choi Y, Kim HS, Kim HO. Comparison of molecular profiles of human mesenchymal stem cells derived from bone marrow, umbilical cord blood, placenta and adipose tissue. Int J Mol Med. 2016;**37**:115–25.
6. Kilroy GE, Foster SJ, Wu X, Ruiz J, Sherwood S, Heifetz A, *et al.* Cytokine profile of human adipose-derived stem cells: Expression of angiogenic, hematopoietic, and pro-inflammatory factors. J Cell Physiol. 2007;**212**:702–9.
7. Tran KV, Gealekman O, Frontini A, Zingaretti MC, Morroni M, Giordano A, *et al.* The vascular endothelium of the adipose tissue gives rise to both white and brown fat cells. Cell Metab. 2012;**15**:222–9.
8. Lin G, Garcia M, Ning H, Banie L, Guo YL, Lue TF, *et al.* Defining stem and progenitor cells within adipose tissue. Stem Cells Dev. 2008;**17**:1053–63.

9. Crisan M, Chen CW, Corselli M, Andriolo G, Lazzari L, Peault B. Perivascular multipotent progenitor cells in human organs. Ann N Y Acad Sci. 2009;**1176**:118–23.
10. Banas A, Teratani T, Yamamoto Y, Tokuhara M, Takeshita F, Osaki M, *et al.* IFATS collection: In vivo therapeutic potential of human adipose tissue mesenchymal stem cells after transplantation into mice with liver injury. Stem Cells. 2008;**26**:2705–12.
11. Rehman J, Traktuev D, Li J, Merfeld-Clauss S, Temm-Grove CJ, Bovenkerk JE, *et al.* Secretion of angiogenic and antiapoptotic factors by human adipose stromal cells. Circulation. 2004;**109**:1292–8.
12. Lee EY, Xia Y, Kim WS, Kim MH, Kim TH, Kim KJ, *et al.* Hypoxia-enhanced wound-healing function of adipose-derived stem cells: Increase in stem cell proliferation and up-regulation of VEGF and bFGF. Wound Repair Regen. 2009;**17**:540–7.
13. Merfeld-Clauss S, Gollahalli N, March KL, Traktuev DO. Adipose tissue progenitor cells directly interact with endothelial cells to induce vascular network formation. Tissue Eng Part A. 2010;**16**:2953–66.
14. Rubina K, Kalinina N, Efimenko A, Lopatina T, Melikhova V, Tsokolaeva Z, *et al.* Adipose stromal cells stimulate angiogenesis via promoting progenitor cell differentiation, secretion of angiogenic factors, and enhancing vessel maturation. Tissue Eng Part A. 2009;**15**:2039–50.
15. Hong SJ, Jia SX, Xie P, Xu W, Leung KP, Mustoe TA, *et al.* Topically delivered adipose derived stem cells show an activated-fibroblast phenotype and enhance granulation tissue formation in skin wounds. PLoS One. 2013;**8**:e55640.
16. Ii M, Horii M, Yokoyama A, Shoji T, Mifune Y, Kawamoto A, *et al.* Synergistic effect of adipose-derived stem cell therapy and bone marrow progenitor recruitment in ischemic heart. Lab Invest. 2011;**91**:539–52.
17. Planat-Benard V, Silvestre JS, Cousin B, Andre M, Nibbelink M, Tamarat R, *et al.* Plasticity of human adipose lineage cells toward endothelial cells: Physiological and therapeutic perspectives. Circulation. 2004;**109**:656–63.
18. Miranville A, Heeschen C, Sengenes C, Curat CA, Busse R, Bouloumie A. Improvement of postnatal neovascularization by human adipose tissue-derived stem cells. Circulation. 2004;**110**:349–55.
19. Park IS, Mondal A, Chung PS, Ahn JC. Vascular regeneration effect of adipose-derived stem cells with light-emitting diode phototherapy in ischemic tissue. Lasers Med Sci. 2015; **30**:533–41.
20. Sumi M, Sata M, Toya N, Yanaga K, Ohki T, Nagai R. Transplantation of adipose stromal cells, but not mature adipocytes, augments ischemia-induced angiogenesis. Life Sci. 2007;**80**: 559–65.
21. Makarevich PI, Boldyreva MA, Gluhanyuk EV, Efimenko AY, Dergilev KV, Shevchenko EK, *et al.* Enhanced angiogenesis in ischemic skeletal muscle after transplantation of cell sheets from baculovirus-transduced adipose-derived stromal cells expressing VEGF165. Stem Cell Res Ther. 2015;**6**:204.
22. Yoshida S, Yoshimoto H, Hirano A, Akita S. Wound healing and angiogenesis through combined use of a vascularized tissue flap and adipose-derived stem cells in a rat hindlimb irradiated ischemia model. Plast Reconstr Surg. 2016;**137**:1486–97.
23. Bekhite MM, Finkensieper A, Rebhan J, Huse S, Schultze-Mosgau S, Figulla HR, *et al.* Hypoxia, leptin, and vascular endothelial growth factor stimulate vascular endothelial cell differentiation of human adipose tissue-derived stem cells. Stem Cells Dev. 2014;**23**:333–51.
24. Kingsbury KJ, Paul S, Crossley A, Morgan DM. The fatty acid composition of human depot fat. Biochem J. 1961;**78**: 541–50.
25. Wood JD, Enser M, Fisher AV, Nute GR, Sheard PR, Richardson RI, *et al.* Fat deposition, fatty acid composition and meat quality: A review. Meat Sci. 2008;**78**:343–58.
26. Bourin P, Bunnell BA, Casteilla L, Dominici M, Katz AJ, March KL, *et al.* Stromal cells from the adipose tissue-derived stromal vascular fraction and culture expanded adipose tissue-derived stromal/stem cells: A joint statement of the International Federation for Adipose Therapeutics and Science (IFATS) and the International Society for Cellular Therapy (ISCT). Cytotherapy. 2013;**15**:641–8.
27. Prasai A, El Ayadi A, Mifflin RC, Wetzel MD, Andersen CR, Redl H, *et al.* Characterization of adipose-derived stem cells following burn injury. Stem Cell Rev. 2017;**13**:781–92.
28. Kalaszczynska I, Ruminski S, Platek AE, Bissenik I, Zakrzewski P, Noszczyk M, *et al.* Substantial differences between human and ovine mesenchymal stem cells in response to osteogenic media: How to explain and how to manage? Biores Open Access. 2013;**2**:356–63.
29. Lyahyai J, Mediano DR, Ranera B, Sanz A, Remacha AR, Bolea R, *et al.* Isolation and characterization of ovine mesenchymal stem cells derived from peripheral blood. BMC Vet Res. 2012;**8**:169.
30. Ito H, Asmussen S, Traber DL, Cox RA, Hawkins HK, Connelly R, *et al.* Healing efficacy of sea buckthorn (Hippophae rhamnoides L.) seed oil in an ovine burn wound model. Burns. 2014;**40**:511–9.
31. Deveci D, Egginton S. Development of the fluorescent microsphere technique for quantifying regional blood flow in small mammals. Exp Physiol. 1999;**84**:615–30.
32. Kondo K, Shintani S, Shibata R, Murakami H, Murakami R, Imaizumi M, *et al.* Implantation of adipose-derived regenerative cells enhances ischemia-induced angiogenesis. Arterioscler Thromb Vasc Biol. 2009;**29**:61–6.
33. Uemura R, Xu M, Ahmad N, Ashraf M. Bone marrow stem cells prevent left ventricular remodeling of ischemic heart through paracrine signaling. Circ Res. 2006;**98**:1414–21.
34. Follin B, Tratwal J, Haack-Sorensen M, Elberg JJ, Kastrup J, Ekblond A. Identical effects of VEGF and serum-deprivation on phenotype and function of adipose-derived stromal cells from healthy donors and patients with ischemic heart disease. J Transl Med. 2013;**11**:219.
35. Wallner C, Abraham S, Wagner JM, Harati K, Ismer B, Kessler L, *et al.* Local application of isogenic adipose-derived stem cells restores bone healing capacity in a type 2 diabetes model. Stem Cells Transl Med. 2016;**5**:836–44.
36. Burmeister DM, Stone R, 2nd, Wrice N, Laborde A, Becerra SC, Natesan S, *et al.* Delivery of allogeneic adipose stem cells in polyethylene glycol-fibrin hydrogels as an adjunct to meshed autografts after sharp debridement of deep partial thickness burns. Stem Cells Transl Med. 2018;**7**: 360–72.
37. Cruz AC, Caon T, Menin A, Granato R, Aragones A, Boabaid F, *et al.* Adipose-derived stem cells decrease bone morphogenetic protein type 2-induced inflammation in vivo. J Oral Maxillofac Surg. 2016;**74**:505–14.

38. Georgiev-Hristov T, Garcia-Arranz M, Garcia-Gomez I, Garcia-Cabezas MA, Trebol J, Vega-Clemente L, *et al.* Sutures enriched with adipose-derived stem cells decrease the local acute inflammation after tracheal anastomosis in a murine model. Eur J Cardiothorac Surg. 2012;**42**:e40–7.
39. Kim JM, Lee ST, Chu K, Jung KH, Song EC, Kim SJ, *et al.* Systemic transplantation of human adipose stem cells attenuated cerebral inflammation and degeneration in a hemorrhagic stroke model. Brain Res. 2007;**1183**:43–50.
40. Shalaby SM, Sabbah NA, Saber T, Abdel Hamid RA. Adipose-derived mesenchymal stem cells modulate the immune response in chronic experimental autoimmune encephalomyelitis model. IUBMB Life. 2016;**68**:106–15.
41. Garimella MG, Kour S, Piprode V, Mittal M, Kumar A, Rani L, *et al.* Adipose-derived mesenchymal stem cells prevent systemic bone loss in collagen-induced arthritis. J Immunol. 2015;**195**:5136–48.
42. Herndon DN, Tompkins RG. Support of the metabolic response to burn injury. Lancet. 2004;**363**:1895–902.
43. Jeschke MG, Boehning DF, Finnerty CC, Herndon DN. Effect of insulin on the inflammatory and acute phase response after burn injury. Crit Care Med. 2007;**35**:S519–23.
44. Schelbergen RF, van Dalen S, ter Huurne M, Roth J, Vogl T, Noel D, *et al.* Treatment efficacy of adipose-derived stem cells in experimental osteoarthritis is driven by high synovial activation and reflected by S100A8/A9 serum levels. Osteoarthritis Cartilage. 2014;**22**:1158–66.
45. Suga H, Glotzbach JP, Sorkin M, Longaker MT, Gurtner GC. Paracrine mechanism of angiogenesis in adipose-derived stem cell transplantation. Ann Plast Surg. 2014;**72**:234–41.
46. Bliley JM, Argenta A, Satish L, McLaughlin MM, Dees A, Tompkins-Rhoades C, *et al.* Administration of adipose-derived stem cells enhances vascularity, induces collagen deposition, and dermal adipogenesis in burn wounds. Burns. 2016;**42**:1212–22.
47. Delle Monache S, Calgani A, Sanita P, Zazzeroni F, Gentile Warschauer E, Giuliani A, *et al.* Adipose-derived stem cells sustain prolonged angiogenesis through leptin secretion. Growth Factors. 2016;**34**:87–96.
48. Pinheiro CH, de Queiroz JC, Guimaraes-Ferreira L, Vitzel KF, Nachbar RT, de Sousa LG, *et al.* Local injections of adipose-derived mesenchymal stem cells modulate inflammation and increase angiogenesis ameliorating the dystrophic phenotype in dystrophin-deficient skeletal muscle. Stem Cell Rev. 2012;**8**:363–74.